JOURNAL OF Materials CHEMISTRY

Photoelectric conversion and second-order optical nonlinearity of Langmuir–Blodgett films of a novel dipolar two-dimensional material

Fu-You Li,[a] Jie Zheng,[b] Lin-Pei Jin,*[a] Xin-Sheng Zhao,[c] Ting-Ting Liu[c] and Jian-Quan Guo[a]

[a]*Department of Chemistry, Beijing Normal University, Beijing 100875, P. R. China*
[b]*State Key Laboratory of Rare Earth Materials Chemistry and Applications, Peking University, Beijing 100871, China*
[c]*Department of Chemistry, Peking University, Beijing 100871, China*

Received 26th October 1999, Accepted 13th March 2000
Published on the Web 18th April 2000

A dipolar two-dimensional multifunctional $(D–\pi)_3–A$ dye molecule, 2,4,6-tris(4-octadecyloxystyryl)pyrylium tetrafluoroborate (OP_3) was synthesized. The dye molecule was successfully transferred onto an ITO electrode or quartz by LB techniques. The second-harmonic generation (SHG) and photoelectric conversion (PEC) properties of monolayers of this "umbrella-molecule" were studied under 10 mN m^{-1} and 30 mN m^{-1} surface pressure. The different tilt angles of the "umbrella-molecules" result in the difference in SHG and PEC properties. Both SHG and PEC properties of OP_3 obtained under 30 mN m^{-1} are better than those obtained under 10 mN m^{-1}.

Introduction

Electrooptic materials are of interest due to their potential applications in electrooptic signals, telecommunications and data storage.[1,2] One of the important components of these materials is a nonlinear optical (NLO) chromophore. Most studies of NLO molecules have focused on dipolar one-dimensional[3,4] and octupolar two- and three-dimensional[5,6] NLO chromophores. Moreover, multifunctional dipolar one-dimensional NLO materials with magnetism,[7] conductivity[8,9] or photoelectric conversion (PEC) properties[10–13] have already been reported. Although dipolar two-dimensional molecules exhibit several interesting properties, however, systematic experimental studies have rarely been done.[14–16] Huang has previously reported a dipolar two-dimensional molecule (P_{3n}) with photoelectric conversion properties.[17] To continue our investigation, we designed a novel dipolar two-dimensional multifunctional $(D–\pi)_3–A$ dye molecule, 2,4,6-tris(4-octadecyloxystyryl)pyrylium tetrafluoroborate (OP_3) (Scheme 1), in which three electron-donating groups link one electron-accepting group through three π-conjugation (-CH=CH-) groups. This OP_3 "umbrella-molecule" could be formed at the air/water interface and was transferred onto an indium–tin oxide (ITO) substrate or quartz by Langmuir–Blodgett (LB) techniques. The second harmonic generation (SHG) and PEC properties of the multifunctional dye LB monolayers were observed.

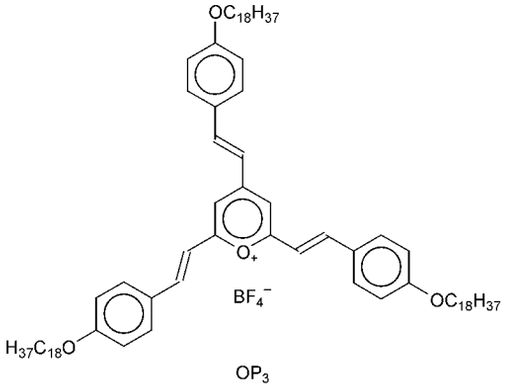

Scheme 1 Molecular structure of the OP_3 dye.

Experimental

4-Octadecyloxybenzaldehyde was prepared according to the method reported previously.[18] 2,4,6-Trimethylpyrylium tetrafluoroborate was synthesized as described in the literature.[19] 2,4,6-Tris(4-octadecyloxystyryl)pyrylium tetrafluoroborate (OP_3) was synthesized by condensing 2,4,6-trimethylpyrylium tetrafluoroborate with three molar equivalents of 4-octadecyloxybenzaldehyde in refluxing absolute ethanol for 5 h. The product was purified by column chromatography (SiO_2, $MeOH–CH_2Cl_2 = 1:12$).

OP_3: yield: 76%, mp: 241–242 °C. Anal. calc. for $C_{83}H_{131}BO_4F_4$: C, 77.87; H, 10.32; found: C, 77.44; H, 10.78%; δ_H (300 MHz, $CDCl_3$): 0.88 (t, 9H, $3CH_3$), 1.26 (m, 78H, $39CH_2$), 1.76 (m, 6H, $3CH_2$), 3.92 (m, 6H, $3OCH_2$), 6.45 (d, 2H, phenyl), 6.72 (d, 4H, phenyl), 6.75 (d, 2H, 2CH=), 6.83 (d, 1H, 1CH=), 6.91 (s, 2H, pyrylium), 7.00 (d, 2H, phenyl), 7.10 (d, 4H, phenyl), 7.18 (d, 2H, 2CH=) and 7.30 (d, 1H, 1CH=).

Methylviologen diiodide (MV^{2+}) was synthesized by reaction of 4,4′-bipyridyl with methyl iodide. Its identity was confirmed by ^{1}HNMR analysis. Hydroquinone (H_2Q) (AR) was recrystallized from water before use. $EuCl_3·6H_2O$ was obtained by reaction of Eu_2O_3 with hydrochloric acid. The electrolyte for the electrochemical experiment was KCl (AR).

Elemental analysis was performed on a Carlo Erba 1106 elemental analyzer. ^{1}HNMR spectra were recorded on a Bruker ARX300 spectrometer. Electronic spectra in solution or on LB films were recorded on a Shimadzu model 3100 UV–VIS–NIR spectrophotometer. Melting points were measured on an X4 micromelting point apparatus. The monolayers of OP_3 were prepared by spreading the OP_3 chloroform solution on an NIMA 622 Langmuir–Blodgett trough (20 ± 1 °C). Water produced by an EASY pure RF system was used as the subphase ($R \sim 18$ MΩ). Details of the methods used for pressure (π)–area (A) measurement and the transfer process

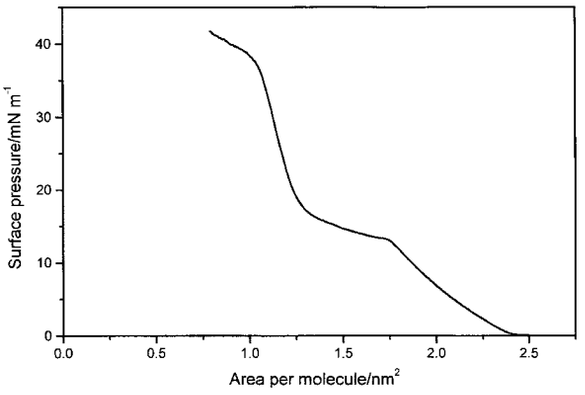

Fig. 1 Surface pressure–area (π–A) isotherms of OP_3 at the air/water interface (20 ± 1 °C).

were the same as described previously.[18] In all cases, the transfer ratios were close to 1.0 ± 0.1.

Second harmonic generation (SHG) experiments were carried out in transmission with the laser beam (Nd:YAG, $\lambda=1064$ nm) at an angle of 45° to the LB films. The SHG data from the LB films were analyzed by the general procedure described by Ashwell.[20] The SHG intensities were calibrated against a Y-cut quartz reference ($d_{11}=0.5$ pm V^{-1}).

Photoelectrochemical measurements were carried out in 0.5 M KCl solution using the LB monolayer-modified ITO electrode, platinum wire and Ag/AgCl electrode as working electrode, counter electrode and reference electrode, respectively. The effective illuminated area of a flat window for OP_3 was 1 cm^{-2}. The incident light beam from a 500 W Xe arc lamp was passed through a group of filters (*ca.* 300–700 nm, Toshiba Co. Japan, and Schott Co. USA) in order to get a given bandpass of light. The light intensity at each wavelength was measured with an energy and power meter (Scientech, USA). The photocurrent was detected using a voltammetric analyzer (CH Instrument, model 600) at ambient temperature.

Results and discussion

LB film properties

The surface pressure *versus* area isotherm of OP_3 is shown in Fig. 1. Data show that the collapse pressure of OP_3 is 38 mN m^{-1}. The isotherm of OP_3 exhibits a characteristic plateau in a broad range of area from 1.75 to 1.30 nm^2 at 13.4 mN m^{-1}. Because the ratio of the area per molecule at the beginning of the plateau to that at its termination amounts to 1.37, we suggest that such a broad plateau is due not to the formation of multilayers but to a conformational rearrangement when the surface pressure reaches 13.4 mN m^{-1}. The limiting areas per molecule of OP_3 before and after the plateau are 2.14 and 1.35 nm^2, respectively, extrapolated from the tangent of the π–A isotherm at 30 mN m^{-1} and 10 mN m^{-1} (Table 1, A). We suggest that the OP_3 is possibly oriented at the air/water interface under different surface pressures as shown in Scheme 2 in which the three electron-donating groups may

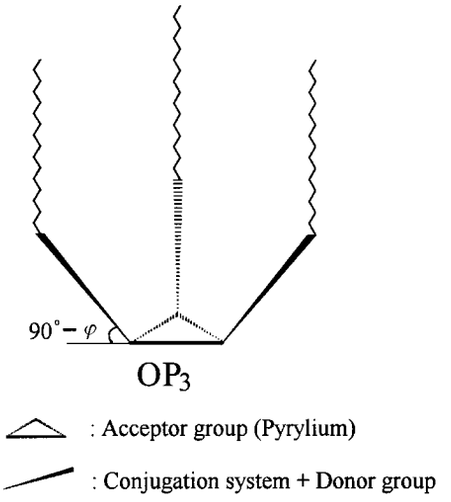

Scheme 2 The possible arrangement of OP_3 at the air/water interface.

be arranged in an umbrella shape on the substrate with different tilt angles φ (relative to the normal line of the substrate). In order to investigate the effect of the surface pressure on the properties of OP_3 LB monolayers, we chose 10 mN m^{-1} and 30 mN m^{-1} which are before and after the plateau in the π–A isotherm as representative pressures. OP_{3H} and OP_{3L} stand for LB monolayers of OP_3 deposited on quartz (or ITO slides) under 30 mN m^{-1} and 10 mN m^{-1}, respectively. Comparing the electronic spectra of OP_{3H} and OP_{3L} LB films with those in chloroform solution (Table 1, λ_{max}), blue-shifts of 63 nm and 55 nm can be observed for OP_{3H} and OP_{3L}, respectively, indicating that H-aggregates formed in the films.[21]

SHG properties

The second order susceptibilities $\chi^{(2)}$ of OP_{3H} and OP_{3L} LB monolayers deposited on quartz are 41 and 11.5 pm V^{-1}, respectively. The tilt angles φ of OP_{3H} and OP_{3L} LB monolayers deposited on quartz are 41° and 70°, respectively. The ratio of the limiting area for OP_{3L} and OP_{3H} (*ca.* 1.58) is approximately equal to the ratio of their cos $(90°-\varphi)$ (*ca.* 1.43), which implies that the difference in the tilt angles for OP_3 and OP_{3L} results mainly from the difference in their limiting areas. The data show that $\chi^{(2)}$ of OP_{3H} is about four times larger than that of OP_{3L}, indicating that the increasing SHG intensity is due not only to the greater density of the molecule (Table 1, No.$_{(m)}$) but also mostly to the change in relative orientation of the chromophores when the surface pressure increases from 10 mN m^{-1} to 30 mN m^{-1}. Therefore, it can be concluded that the change in relative orientation of the chromophores is an important factor for the SHG properties.

Photoelectric conversion properties (PEC)

A steady cathodic photocurrent was obtained from the OP_{3H} and OP_{3L} monolayer-modified ITO electrode in 0.5 M KCl solution under illumination with 137 mW cm^{-2} white light. In

Table 1 Properties of OP_{3H} and OP_{3L} LB films[a]

Dye	I^b/nA cm^{-2}	I^c/nA cm^{-2}	η^c(%)	I^d/nA cm^{-2}	η^d(%)	$\chi^{(2)}$/pm V^{-1}	φ/°	A/nm^2	No.$_{(m)}$/10^{13} cm^{-2}	$I_1{}^b/10^{-12}$ nA molecule^{-1}	$\lambda_{max(sol)}$/nm	$\lambda_{max(f)}$/nm
OP_{3H}	158	12	0.13	89	0.96	41	41	1.35	7.41	2.13	501	438
OP_{3L}	70	5.0	0.06	27.5	0.33	11.5	70	2.14	4.67	1.50	501	446

[a] I: photocurrent per square centimetre; I_1: photocurrent per molecule; η: external quantum yield; $\chi^{(2)}$: second order susceptibility; ϕ: tilt angle relative to the normal line on the substrate; A: limiting area per molecule; No.$_{(m)}$: molecule number per square centimetre. [b] Irradiation under 137 mW cm^{-2} white light for OP_{3H} and OP_{3L} in 0.5 M KCl electrolyte solution containing dissolved O_2. [c] Irradiation under 137 mW cm^{-2} white light at 450 nm for OP_{3H} and OP_{3L}, respectively, in 0.5 M KCl electrolyte solution containing dissolved O_2. [d] Irradiation under 137 mW cm^{-2} white light at 450 nm for OP_{3H} and OP_{3L}, respectively, under -100 mV, dissolved O_2, 3 mM MV^{2+} and 4 mM Eu^{3+}.

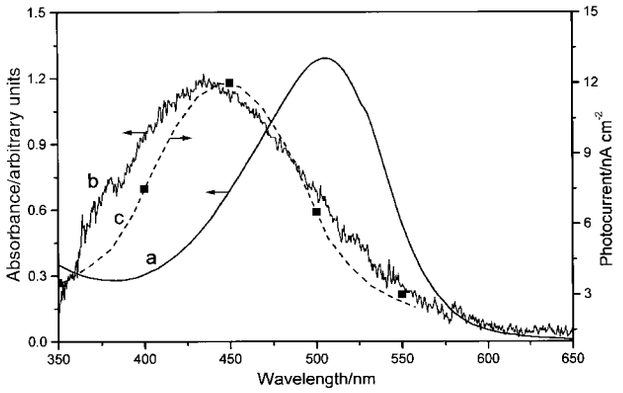

Fig. 2 UV–Vis absorption spectra of OP_{3H} in chloroform solution (a) and on LB monolayers (b) and action spectrum (c) of the cathodic photocurrents for OP_{3H}. The intensities of different wavelengths are all normalised.

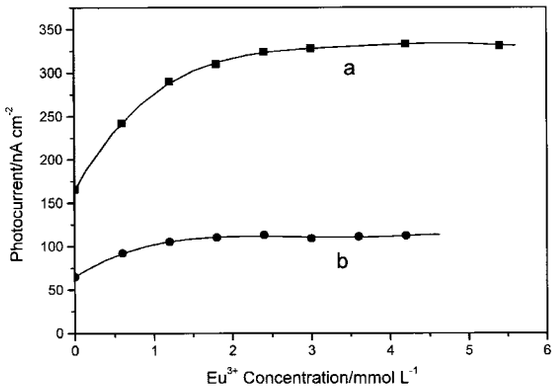

Fig. 3 Dependence of the photocurrent on the concentration of $EuCl_3$ under ambient conditions for OP_{3H} (a) and OP_{3L} (b) monolayer upon irradiation with 137 mW cm^{-2} white light.

this discussion, OP_{3H} is taken as an example for convenience. The agreement between the photocurrent spectrum of the cathodic photocurrent and the absorption spectrum for OP_{3H} (see Fig. 2) indicates that the aggregates of OP_{3H} in the LB monolayer are responsible for photocurrent generation. About 12 nA cm^{-2} cathodic photocurrent can be obtained for OP_{3H} under irradiation at 450 nm (3.48×10^{15} photons cm^{-2} s^{-1}) under ambient conditions, corresponding to a quantum yield of 0.13% (Table 1, η) (the absorbance of the film is about 0.7% at 450 nm).

It is well known that the intensity (even the direction) of the photocurrent depends on the nature of the redox couple in the aqueous phase surrounding the electrode. The effects of electron donors and acceptors on the cathodic photocurrent for OP_{3H} and OP_{3L} show that electron acceptors (MV^{2+}, Eu^{3+} and O_2) sensitize the cathodic photocurrent and electron donors (H_2Q and N_2) quench it (even reverse it) and all level off at a certain concentration (Table 2). For example, it can be seen from Fig. 3 that the cathodic photocurrent increases gradually with increasing concentration of $EuCl_3$ and levels off at 4.0 mmol dm^{-3}. Under favorable conditions, such as irradiation under a 137 mW cm^{-2} white light at 450 nm, with -100 mV bias voltage, dissolved O_2, 4 mM Eu^{3+} and 3 mM MV^{2+}, the quantum yields for OP_{3H} and OP_{3L} were 0.96% and 0.33%, respectively (Table 1).

To understand the effect of bias voltage on photoinduced electron injection, the relationship between bias voltage and PEC was investigated. Fig. 4 shows the dependence of photocurrent on bias voltage. Results show that the cathodic photocurrents for both OP_{3H} and OP_{3L} increase as the negative bias voltage of the electrode increases, indicating that the photocurrent flows in the same direction as the applied negative voltage. With reference to the effects of saturated dissolved O_2 and addition of the electron donor and acceptor in electrolyte solution on the photoelectric conversion behaviors, a possible

Table 2 Effect of donors and acceptors on the photoelectric conversion of OP_{3H} monolayer LB film mdified-ITO electrode

		Photocurrent[a]/nA cm^{-2}	
Donor/acceptor	Concn./mM	Ambient	N_2 degassed
MV^{2+}	0	150	30
	3.5	330	114
Eu^{3+}	0	166	35
	4.2	381	147
H_2Q	0	162	33
	4.8	−285[b]	−840

[a]Irradiation under 137 mW cm^{-2} white light for OP_{3H} in 0.5 M KCl electrolyte solution. [b]"−" indicates anodic photocurrent.

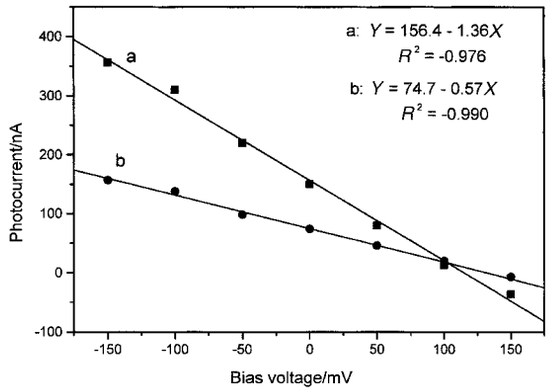

Fig. 4 Photocurrent *versus* bias voltage for OP_{3H} and OP_{3L} LB monolayer film modified ITO electrodes in 0.5 M KCl aqueous solution under ambient conditions, upon irradiation with 137 mW cm^{-2} white light.

electron transfer mechanism for OP_{3H} (as an example) is proposed as shown in Scheme 3. In the presence of some electron acceptors, such as dissolved O_2, MV^{2+} or Eu^{3+} in electrolyte solution, an electron transfers from the excited state of OP_{3H} to the electron acceptor, and subsequently an electron of the ITO conduction band injects into the hole residing in the dye aggregate. Thus, a cathodic photocurrent is generated. On the contrary, if there is a strong electron donor (such as H_2Q) in the system, both ITO and H_2Q compete to donate an electron to the LB aggregate, so it will exhibit a reduced cathodic photocurrent or even reverse the direction of the photocurrent.

Conclusions

Taking the limiting area per molecule into account, one can get the molecular numbers per square centimetre for OP_{3H} and OP_{3L} (Table 1), 7.41×10^{13} and 4.67×10^{13}, respectively. With

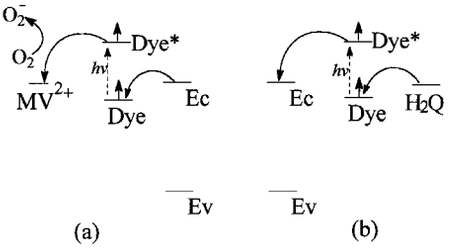

Scheme 3 Schematic diagram showing electron transfer processes. (a) cathodic photocurrent; (b) anodic photocurrent. Dye and Dye* represent the ground state and excited states of the dye OP_{3H}, respectively.

reference to the photocurrent per square centimetre, it is easy to get photocurrent per molecule for OP_{3H} and OP_{3L}, 2.13×10^{-12} and 1.50×10^{-12} nA molecule^{-1}, respectively. Therefore, the photocurrent per OP_{3H} molecule is about 1.42 times larger than that of OP_{3L}. Although the number of active moieties per area in the LB films is an important factor contributing to the photoelectric conversion performance, however, in this case, the better PEC behavior of OP_{3H} (30 mN m^{-1}) than OP_{3L} (10 mN m^{-1}) is mainly due not to the greater number of molecules per square centimetre but to the decreasing tilt angle (relative to the normal line of the substrate) of OP_{3H}. Therefore, it can be concluded that the relative orientation change of the chromophores plays an important role in PEC and SHG properties.

Acknowledgements

The authors thank the State Key Project of Fundamental Research (G1998061300) and National Natural Science Foundation of China (29671001, 29671003) for financial support of this work.

References

1 A. Miller, K. R. Welford and B. Daino, *Nonlinear optical materials and devices for applications in the information technology*, Kluwer Academic Publishers, Dordrecht, The Netherlands, 1993.
2 S. R. Marder, B. Kippelen, A. K.-Y. Jen and N. Peyghambarian, *Nature*, 1997, **388**, 845.
3 L. T. Cheng, W. Tam, S. H. Stevenson, G. R. Meridith, G. Rikken and S. R. Marder, *J. Phys. Chem.*, 1991, **95**, 10631.
4 D. R. Kanis, M. A. Ratner and T. J. Marks, *Chem. Rev.*, 1994, **94**, 195.
5 J. Zyss, *Nonlinear Opt.*, 1991, **1**, 3.
6 J. Zyss and I. Ledoux, *Chem. Rev.*, 1994, **94**, 77.
7 P. G. Lacroix, R. Clément, K. Nakatani, J. Zyss and I. Ledoux, *Science*, 1994, **263**, 658.
8 P. G. Lacroix and K. Nakatani, *Adv. Mater.*, 1997, **9**, 1105.
9 R. Andreu, I. Malfanr, P. G. Lacroix and H. Gornitzka, *Chem. Mater.*, 1999, **11**, 830.
10 J. Zhai, C. H. Huang, T. X. Wei, A. C. Yu and X. S. Zhao, *Solid State Commun.*, 1999, **109**, 733.
11 W. S. Xia, C. H. Huang and D. J. Zhou, *Langmuir*, 1997, **13**, 80.
12 A. D. Lang, J. Zhai, C. H. Huang, L. B. Gan, Y. L. Zhao, D. J. Zhou and Z. D. Chen, *J. Phys. Chem. B*, 1998, **102**, 1424.
13 D. G. Wu, C. H. Huang, Y. Y. Huang, L. B. Gan, A. C. Yu, L. M. Ying and X. S. Zhao, *J. Phys. Chem. B*, 1999, **103**, 7130.
14 H. S. Nalwa, T. Watanabe and S. Miyata, *Adv. Mater.*, 1995, **7**, 754.
15 R. Wortmann, P. Krämer, C. Glania, S. Lebus and N. Detzer, *Chem. Phys.*, 1993, **173**, 99.
16 S. Brasselet and J. Zyss, *J. Nonlinear Opt. Phys. Mater.*, 1996, **5**, 671.
17 D. G. Wu, C. H. Huang, L. B. Gan, W. Zhang, J. Zheng, H. X. Luo and N. Q. Li, *J. Phys. Chem. B*, 1999, **103**, 4377.
18 D. G. Wu, C. H. Huang, L. B. Gan and Y. Y. Huang, *Langmuir*, 1998, **14**, 3783.
19 H. Hauser and H. Kaiser, *Org. Synth.*, 1973, **Coll. Vol. 5**, 1112.
20 G. J. Ashwell, P. D. Jackson, D. Lochum, W. A. Crossland, P. A. Thrompson, G. S. Bahra, C. R. Brown and C. Jasper, *Proc. R. Soc. London A*, 1994, **445**, 385.
21 W. F. Mooney, P. E. Brown, J. C. Russell, S. B. Costa, L. G. Pedersen and D. G. Whitten, *J. Am. Chem. Soc.*, 1984, **106**, 5659.